Mathematica Pannonica
20/2 (2009), 167–187

CLASSIFICATION OF SYMMETRY GENERATING POLYGON-TRANSFORMATIONS AND GEOMETRIC PRIME ALGORITHMS

Dimitris **Vartziotis**

NIKI Ltd. Digital Engineering, Research Center, 205 Ethnikis Antistasis Street, 45500 Katsika, Ioannina, Greece

TWT GmbH Science & Innovation, Research Department, Bernhäuser Straße 40–42, 73765 Neuhausen, Germany

Joachim **Wipper**

TWT GmbH Science & Innovation, Research Department, Bernhäuser Straße 40–42, 73765 Neuhausen, Germany

Received: October 2008

MSC 2000: 11 A 51, 11 N 35, 51 M 04, 52 B 15

Keywords: Napoleon's theorem, polygon transformation, eigenpolygon, circulant matrix, prime number, prime factorization, geometric sieve.

The primes are stars.

Abstract: Infinite polygon transformations by iteratively taking the apices of similar isosceles triangles erected on the sides of a polygon are analyzed. In contrast to other approaches, this is done with respect to the base angle of the isosceles triangles. A finite set of characteristic angles is derived, which only depend on the number of vertices of the polygon. This results in a systematic and complete classification of consecutive base angle intervals and the associated limit polygons. The latter in turn are linear combinations of eigenpolygons obtained by diagonalizing the circulant matrix representation of the transformation. Analyzing the principles of the symmetry of eigenpolygons and thereby of the limit polygons reveals a connection to prime numbers. Based on these results, a geometric sieve as well as a factorization algorithm for prime numbers is presented.

E-mail address (corresponding author): dimitris.vartziotis@nikitec.gr

1. Introduction

The construction of similar figures on the sides of a polygon and the resulting concentric polygons has fascinated mathematicians for over a century [6]. The most popular theorem in this area is Napoleon's Theorem [19] where a regular triangle is constructed within one transformation step by connecting the centers of equilateral triangles erected on each side of the initial triangle. Since then, this approach has been generalized with respect to the number of vertices of the initial polygon, the geometric construction schemes, the resulting symmetries, or the number of transformation steps [3, 10, 14, 20]. One example is the Petr–Douglas–Neumann theorem [5], which transforms an n-gon within $n-2$ steps into an equilateral polygon. Another class of transformation schemes uses an infinite number of iteration steps [11, 12, 20].

This paper adopts the conjectures concerning the relation between polygon transformations and prime numbers given by [13] and provides a mathematical foundation. In the following, this modified polygon transformation will be analyzed. On each side of the polygon, similar isosceles triangles are erected. After that, the apices of these similar triangles are connected, which results in a new polygon. In contrast to existing approaches, the sequence resulting from iteratively applying the same transformation will be analyzed with respect to the base angle $\theta \in (0, \pi/2)$ of the isosceles triangles. This is illustrated in Fig. 1 for random initial polygons with $n = 10$ vertices (upper) and $n = 11$ vertices (lower).

It will be shown that there is a change in the geometry of limit figures of the sequences of scaled polygons at each characteristic angle $\theta_k = \pi(2k+1)/(2n)$, $k \in \{0, \ldots, \lfloor n/2 \rfloor - 1\}$, leading to a full classification of limit polygons as depicted in Fig. 1. Whereas the polygons for θ within an interval bounded by characteristic angles are regular polygons or equilateral stars with possibly multiple vertices (positioned above the center of the according interval), the polygons for $\theta = \theta_k$, $k > 0$, are linear combinations of the neighboring limit polygons. Furthermore, the unscaled polygons degenerate to their common centroid, become bounded regular n-gons or grow infinitely in the case of θ being smaller, equal or larger than $\theta_0 = \pi/(2n)$.

A proof is given that n is a prime number if, and only if, all except the first two resulting polygons for angles within the intervals bounded by characteristic angles are star shaped n-gons. Otherwise, reduced poly-

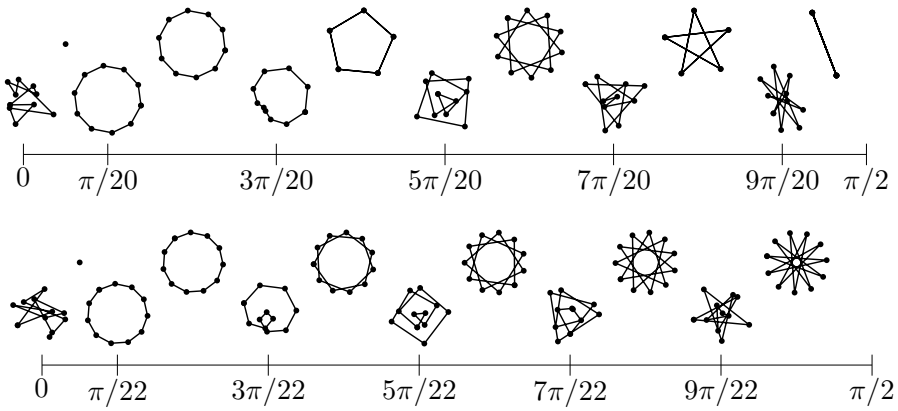

Figure 1: Initial random polygons (plotted above $\theta = 0$) and resulting limit polygons for $n = 10$ (upper) and $n = 11$ (lower) depending on the base angle $\theta \in (0, \pi/2)$.

gons with vertex multiplicities greater than one occur. This results in a geometric factorization algorithm and sieve for prime numbers.

In this paper, a representation of the transformation using complex numbers and circulant matrices is given. By analyzing the transformation using the discrete Fourier transform, the characteristic angles are derived and it will be shown that the obtained shapes are linear combinations of specific eigenpolygons also known as fundamental polygons [1, 7]. Furthermore, analyzing the symmetries of eigenpolygons reveals their connection to prime numbers.

2. Transformation of a polygon

First, a definition of the transformation of a polygon using complex numbers will be given. Let $z^{(0)} \in \mathbb{C}^n$ denote a plane counterclockwise oriented polygon with $n \geq 3$ vertices $z_k^{(0)} := (z^{(0)})_k$, $k \in \{0, \ldots, n-1\}$, and sides of length > 0, which may possibly intersect each other. Over each side $z_k^{(0)} z_{(k+1) \bmod n}^{(0)}$ of the polygon an outward directed isosceles triangle $z_k^{(0)} z_k^{(1)} z_{(k+1) \bmod n}^{(0)}$ with base angle $\theta \in (0, \pi/2)$ is constructed, as depicted in Fig. 2.

The apices are given by

$$z_k^{(1)} := w z_k^{(0)} + \overline{w} z_{(k+1) \bmod n}^{(0)} \quad \text{with} \quad w := \frac{1}{2}(1 + \mathrm{i} \tan\theta)$$

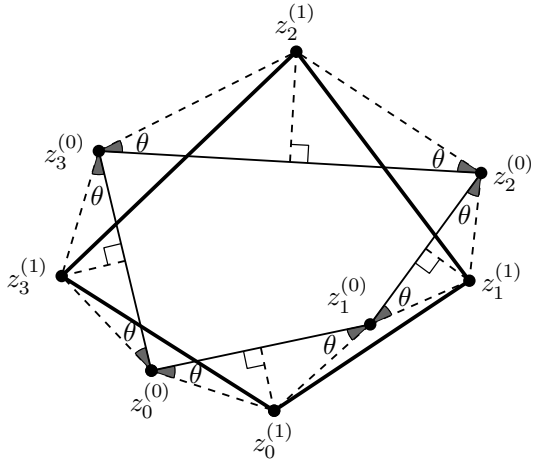

Figure 2: Transformation of a polygon in the case of $n = 4$ using $\theta = \pi/6$.

and $\overline{w}$ denoting the complex conjugate of w. The vertices $z_k^{(1)}$ in term define a new polygon $z^{(1)}$, which can be obtained by using the following matrix formulation.

Definition 2.1. The linear transformation of a polygon $z^{(\ell)} \in \mathbb{C}^n$ into a new polygon $z^{(\ell+1)} \in \mathbb{C}^n$ is given by

$$z^{(\ell+1)} = \begin{pmatrix} z_0^{(\ell+1)} \\ z_1^{(\ell+1)} \\ \vdots \\ z_{n-2}^{(\ell+1)} \\ z_{n-1}^{(\ell+1)} \end{pmatrix} := \underbrace{\begin{pmatrix} w & \overline{w} & & & \\ & w & \overline{w} & & \\ & & \ddots & \ddots & \\ & & & w & \overline{w} \\ \overline{w} & & & & w \end{pmatrix}}_{=:M} \begin{pmatrix} z_0^{(\ell)} \\ z_1^{(\ell)} \\ \vdots \\ z_{n-2}^{(\ell)} \\ z_{n-1}^{(\ell)} \end{pmatrix} = M z^{(\ell)}\,, \tag{1}$$

where $w = (1 + \mathrm{i}\tan\theta)/2$.

Due to $w + \overline{w} = 1$, the sum of each row and column of M is one, thus leading to the familiar result that the transformation preserves the centroid of the polygon. That is, $\frac{1}{n}\sum_{k=0}^{n-1} z_k^{(\ell+1)} = \frac{1}{n}\sum_{k=0}^{n-1} z_k^{(\ell)}$, which can easily be shown by rearranging the sum and collecting the coefficients of $z_k^{(\ell)}$.

Iteratively applying the transformation given by Def. 2.1 to an initial polygon $z^{(0)}$ leads to a sequence of concentric polygons $z^{(\ell)}$, $\ell \in \mathbb{N}$, with $z^{(\ell)} = M^\ell z^{(0)}$. This is depicted in Fig. 3 for different transformation angles θ and iteration numbers ℓ. In this, the same initial 10-gon $z^{(0)}$

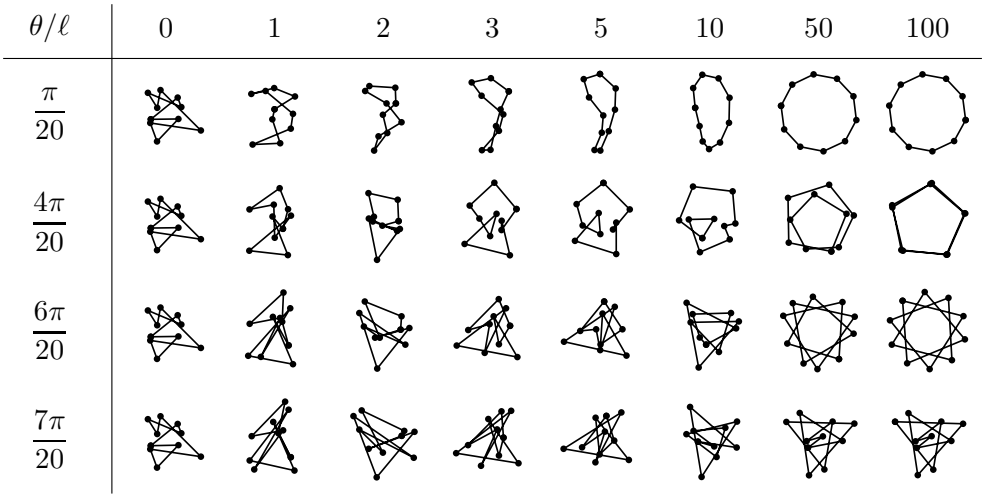

Figure 3: Sequences of polygons $z^{(\ell)} = M^\ell z^{(0)}$ obtained by iteratively applying the transformation using different transformation angles θ.

as depicted on the upper left of Fig. 1 has been used. Additionally, the polygon size has been normalized after each iteration step, to avoid the rapid increase of size in the case of larger θ values. In order to determine the convergence behavior of such sequences, the matrix M will be analyzed in the following.

3. Eigenvalues and eigenpolygons

Since each row of M is a cyclic shift of its preceeding row, the theory of circulant matrices can be applied. For the convenience of the reader, the relevant results will be given briefly (cf. for example [2, 4]).

The square matrix $A \in \mathbb{C}^{n\times n}$ is called circulant, if it is of the form

$$A := \begin{pmatrix} a_0 & a_1 & \dots & a_{n-1} \\ a_{n-1} & a_0 & \dots & a_{n-2} \\ \vdots & \vdots & \ddots & \vdots \\ a_1 & a_2 & \dots & a_0 \end{pmatrix}.$$

It is fully defined by its first row vector $a := (a_0, \dots, a_{n-1})$ with zero-based element indices. With $r := \exp(2\pi\mathrm{i}/n)$ denoting the n-th root of unity it holds that A is diagonalized by the unitary discrete Fourier-Matrix

$$F := \frac{1}{\sqrt{n}} \begin{pmatrix} r^{0\cdot 0} & \dots & r^{0\cdot(n-1)} \\ \vdots & \ddots & \vdots \\ r^{(n-1)\cdot 0} & \dots & r^{(n-1)\cdot(n-1)} \end{pmatrix}$$

with entries $f_{\mu,\nu} = r^{\mu\cdot\nu}/\sqrt{n}$ and likewise zero-based indices $\mu, \nu \in$ $\in \{0, \dots, n-1\}$. That is, the diagonal matrix D of the eigenvalues η_k, $k \in \{0, \dots, n-1\}$, is given by

$$D = \operatorname{diag}(\eta_0, \dots, \eta_{n-1}) := F^* A F\,, \tag{2}$$

with F^* denoting the conjugate transpose of F. Furthermore, the vector $\eta := (\eta_0, \dots, \eta_{n-1})^{\mathrm{t}}$ of all eigenvalues can be easily computed by multiplying the non-normalized Fourier-Matrix with the transposed first row of A, i.e. $\eta = \sqrt{n} F a^{\mathrm{t}}$.

In the case of the geometric transformation M given in the previous section it holds that $a = (w, \overline{w}, 0, \dots, 0)$. And like w the eigenvalues η_k depend on the base angle θ. But in order to simplify the notation, η_k will be used instead of $\eta_k(\theta)$.

Lemma 3.1. *The eigenvalues of the iteration matrix M according to* (1) *are given by*

$$\eta_k = w + r^k \overline{w} = \sec\theta \cos\left(\theta - \frac{\pi k}{n}\right) \mathrm{e}^{\mathrm{i}\pi k/n}\,, \tag{3}$$

where $k \in \{0, \dots, n-1\}$. In particular it holds that $\eta_0 = 1$.

Proof. Since the representation $\eta_k = w + r^k \overline{w}$ follows readily from $\eta = \sqrt{n} F (w, \overline{w}, 0, \dots, 0)^{\mathrm{t}}$ and the definition of F, only the second representation has to be shown.

Due to $\theta \in (0, \pi/2)$, it holds that $|w| = \frac{1}{2}\sqrt{1 + \tan^2\theta} = \frac{1}{2}\sec\theta$. Furthermore, the argument of w is given by θ and that of r^k by $2\pi k/n$. Collecting the real and imaginary parts of the two summands in $\eta_k =$ $= w + r^k \overline{w}$ and applying trigonometric identities to the following expressions in squared brackets results in

$$\eta_k = \frac{1}{2}\sec\theta \left(\left[\cos\theta + \cos\left(\frac{2\pi k}{n} - \theta\right) \right] + \mathrm{i} \left[\sin\theta + \sin\left(\frac{2\pi k}{n} - \theta\right) \right] \right) =$$
$$= \sec\theta \cos\left(\theta - \frac{\pi k}{n}\right) \left(\cos\frac{\pi k}{n} + \mathrm{i} \sin\frac{\pi k}{n} \right),$$

which implies (3). The special case $\eta_0 = 1$ follows likewise from (3) or $\eta_0 = w + \overline{w} = 2\operatorname{Re} w = 1$. $\diamondsuit$

The fact that all circulant matrices are diagonalizable by the same Fourier matrix F is remarkable and has far reaching consequences with respect to resulting symmetries. Hence, the orthonormal vectors given by the columns

$$f_k := (f_{0,k}, \dots, f_{n-1,k})^{\mathrm{t}} = \frac{1}{\sqrt{n}} \left(r^{0\cdot k}, r^{1\cdot k}, \dots, r^{(n-1)\cdot k}\right)^{\mathrm{t}},$$

$k \in \{0, \dots, n-1\}$, of F build a natural basis for the analysis of circulant polygon transformations. The vectors f_k can also be interpreted as polygons, which will be called *Fourier polygons*.

The coefficients c_k in the representation of $z^{(0)} = \sum_{k=0}^{n-1} c_k f_k$ in terms of the Fourier polygons are given by the entries of the vector $c := F^* z^{(0)}$. Furthermore, due to (2) the transformation matrix M can be written as $M = FDF^*$ with D denoting the diagonal matrix of the eigenvalues η_k. Hence, the polygon obtained by successively applying ℓ transformation steps can be written as

$$z^{(\ell)} = M^\ell z^{(0)} = (FDF^*)^\ell z^{(0)} = FD^\ell F^* z^{(0)} = FD^\ell c = \sum_{k=0}^{n-1} \eta_k^\ell c_k f_k \,. \tag{4}$$

That is, $z^{(\ell)}$ is a linear combination of the n polygons $c_k f_k$ scaled by the ℓ-th power of the associated eigenvalues. Therefore, this special polygons will be defined and analyzed below.

Definition 3.1. For $k \in \{0, \dots, n-1\}$ the n-dimensional complex vector

$$v_k := c_k f_k = \frac{\left(F^* z^{(0)}\right)_k}{\sqrt{n}} \left(r^{0\cdot k}, \dots, r^{(n-1)\cdot k}\right)^{\mathrm{t}} \tag{5}$$

will be called the k-th eigenpolygon of the initial polygon $z^{(0)}$.

Due to $f_0 = \frac{1}{\sqrt{n}}(1, \dots, 1)^{\mathrm{t}}$ and $\left(F^* z^{(0)}\right)_0 = \frac{1}{\sqrt{n}} \sum_{k=0}^{n-1} z_k^{(0)}$, each vertex of the associated degenerated eigenpolygon v_0 is $\frac{1}{n} \sum_{k=0}^{n-1} z_k^{(0)}$ representing the centroid of $z^{(0)}$. Furthermore, due to $\eta_0 = 1$ and the decomposition (4) it holds that

$$z^{(\ell)} = \sum_{k=0}^{n-1} \eta_k^\ell v_k = v_0 + \sum_{k=1}^{n-1} \eta_k^\ell v_k \,. \tag{6}$$

It should be noted that the eigenpolygons v_k do not necessarily form a basis of $\mathbb{C}^n$, since some of the coefficients c_k might be zero causing the

associated v_k to become zero vectors. However, since $\eta_0 = 1$ in contrast to all other eigenvalues does not depend on the base angle θ, v_o representing the centroid is always preserved as can be seen by equation (6).

Since all circulant $(n \times n)$-matrices can be diagonalized by the same Fourier matrix F, all geometric transformations represented by such matrices lead to the same eigenpolygons. Therefore, the eigenpolygons do not depend on the base angle θ, but only on the initial polygon $z^{(0)}$. Hence, different transformation schemes result in different eigenvalues thus placing emphasis on different symmetric configurations.

Since the eigenpolygon v_k is the Fourier polygon f_k times the coefficient $c_k \in \mathbb{C}$, v_k preserves the symmetry of the f_k. This will be stated more precisely in the following lemma, since this symmetry is also reflected by the limit polygons of the iterated transformation.

Lemma 3.2. *For $k, \mu \in \{0, \ldots, n-1\}$ it holds that*

$$(v_k)_\mu = r^{\mu k}(v_k)_0\,, \tag{7}$$

that is, the μ-th vertex of the eigenpolygon v_k can be derived by rotating the first vertex by angle $2\pi\mu k/n$. In particular it follows that $(v_k)_{\mu \bmod n} = = r^k(v_k)_{\mu-1}$ where $\mu \in \{1, \ldots, n\}$.

Proof. This follows readily from equation (5) since

$$(v_k)_\mu = c_k(f_k)_\mu = c_k \left(\frac{1}{\sqrt{n}}\, r^{\mu k} \right) = r^{\mu k} \left(\frac{c_k}{\sqrt{n}} \cdot 1 \right) = r^{\mu k}(v_k)_0\,.$$

The rotation angle can be derived from $r^{\mu k} = \exp(2\pi \mathrm{i} \mu k/n)$ and the representation $(v_k)_{\mu \bmod n} = r^k(v_k)_{\mu-1}$ is implied by equation (7). $\Diamond$

If ℓ tends to infinity, $z^{(\ell)}$ tends to the scaled eigenpolygon belonging to the eigenvalue with the largest absolute value. Using (3) in order to determine the dominating eigenvalue implies

$$|\eta_k| = \sec\theta \left| \cos\left(\theta - \frac{\pi k}{n} \right) \right|\,.$$

Fig. 4 depicts the values of $|\eta_k|$ depending on $\theta \in (0, \pi/2)$ for $k \in \{0, \ldots, n-1\}$ in the case of $n \in \{5, 6\}$. One can observe that intersections of the functions $|\eta_k|$ occur only at angles θ which are multiples of $\pi/(2n)$. This is stated by the following lemma.

Lemma 3.3. *For $k, m \in \{0, \ldots, n-1\}$, $k \neq m$, the functions $|\eta_k|$ and $|\eta_m|$ of $\theta \in (0, \pi/2)$ may only intersect for $\theta = \mu\pi/(2n)$ where $\mu \in \{1, \ldots, n-1\}$.*

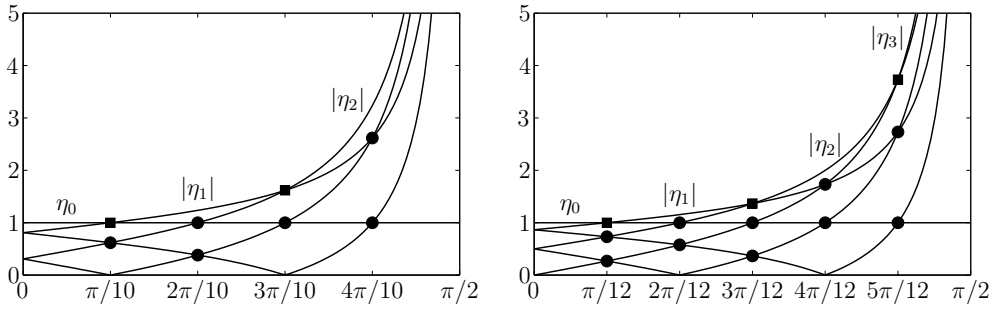

Figure 4: Absolute values of eigenvalues for $\theta \in (0, \pi/2)$ in the case of $n = 5$ (left) and $n = 6$ (right). Dominating eigenvalues are named.

Proof. Since $|\eta_k|$ and $|\eta_m|$ are positive, this will be shown by analyzing the roots of the difference function of the squared values

$$(8)\quad d_{k,m}(\theta) := |\eta_k|^2 - |\eta_m|^2 = \sec^2\theta \left(\cos^2\left(\theta - \frac{\pi k}{n}\right) - \cos^2\left(\theta - \frac{\pi m}{n}\right)\right) =$$

$$= \sec^2\theta \, \sin\left(2\theta - \pi\,\frac{k+m}{n}\right) \sin\left(\pi\,\frac{k-m}{n}\right).$$

Since $|k-m|/n \in \{1/n, \ldots, (n-1)/n\}$, roots can only occur, if the argument of the first sine factor in (8) is a multiple of π, that is

$$2\theta - \pi\frac{k+m}{n} = \nu\pi \quad \Leftrightarrow \quad \theta = \frac{\pi}{2}\left(\nu + \frac{k+m}{n}\right), \quad \nu \in \mathbb{Z}\,.$$

Due to $\theta \in (0, \pi/2)$, the factor $\nu + (k+m)/n$ has to be in $(0,1)$ thus implying $k+m \neq n$ and $\nu = -\lfloor (k+m)/n \rfloor$, where $\lfloor \cdot \rfloor$ denotes rounding towards zero. Since $k \neq m$, this results in $(k+m) \in \{1, \ldots, 2n-3\} \setminus \{n\}$.

In the case of $(k+m) \in \{1, \ldots, n-1\}$ and $(k+m) \in \{n+1, \ldots, 2n-3\}$ it follows that $\nu = 0$ and $\nu = -1$ respectively, thus providing the roots

$$\theta = \frac{\pi}{2n}(k+m) \quad \text{and} \quad \theta = \frac{\pi}{2n}(k+m-n)$$

respectively, as stated in the lemma. $\Diamond$

The behavior of $z^{(\ell)}$ depends on the dominating eigenvalue, which itself depends on the base angle θ. As can be seen in Fig. 4, the dominating eigenvalue changes at each odd multiple of $\pi/(2n)$ marked by square markers. This is stated by the following lemma, which also gives the index of the dominating eigenvalue for each interval.

Lemma 3.4. *For $k \in \{0, \dots, \lfloor n/2 \rfloor - 1\}$, where $\lfloor \cdot \rfloor$ denotes rounding towards zero, let*

$$\theta_k := \frac{\pi}{2n}(2k+1)\,, \quad \textit{furthermore} \quad \theta_{-1} := 0, \quad \theta_{\lfloor n/2 \rfloor} := \frac{\pi}{2}\,. \tag{9}$$

On each interval (θ_{k-1}, θ_k), $k \in \{0, \dots, \lfloor n/2 \rfloor\}$, the index of the dominating eigenvalue is given by k, that is

$$\theta \in (\theta_{k-1}, \theta_k) \quad \Rightarrow \quad |\eta_k| > |\eta_m| \quad \forall m \in \{0, \dots, n-1\} \setminus \{k\}\,. \tag{10}$$

In addition, for $k \in \{0, \dots, \lfloor n/2 \rfloor - 1\}$

$$\theta = \theta_k \quad \Rightarrow \quad |\eta_k| = |\eta_{k+1}| > |\eta_m| \quad \forall m \in \{0, \dots, n-1\} \setminus \{k, k+1\}\,, \tag{11}$$

that is, for $\theta = \theta_k$ the function $|\eta_k|$ is only intersected by $|\eta_{k+1}|$.

Proof. Induction over the intervals (θ_{k-1}, θ_k) for $k \in \{0, \dots, \lfloor n/2 \rfloor\}$ will be used. In the case of $k = 0$ implying $\theta \in (\theta_{-1}, \theta_0) = \big(0, \pi/(2n)\big)$ equation (10) holds, if the associated difference function $d_{0,m}(\theta)$ according to (8) is positive for all $m \in \{1, \dots, n-1\}$. This is the case, since

$$d_{0,m}(\theta) = \underbrace{\sec^2\theta}_{>0} \underbrace{\sin\left(2\theta - \pi\,\frac{m}{n}\right)}_{<0} \underbrace{\sin\left(\pi\,\frac{-m}{n}\right)}_{<0} > 0\,,$$

due to $\sec^2\theta > 0$ in the case of the first factor, $-\pi < 2 \cdot 0 - \pi\frac{n-1}{n} < < 2\theta - \pi\frac{m}{n} < 2\frac{\pi}{2n} - \pi\frac{1}{n} = 0$ in the case of the second factor, and $-\pi\frac{m}{n} \in (-\pi, 0)$ in the case of the third factor.

In order to show (11) the equation

$$d_{0,m}\left(\frac{\pi}{2n}\right) = \underbrace{\sec^2\frac{\pi}{2n}}_{\neq 0} \sin\left(\frac{\pi}{n} - \pi\frac{m}{n}\right) \underbrace{\sin\left(\pi\frac{-m}{n}\right)}_{\neq 0} \stackrel{!}{=} 0$$

implies $\frac{\pi}{n} - \pi\frac{m}{n} = \pi\frac{1-m}{n} \stackrel{!}{=} \nu\pi$ with $\nu \in \mathbb{Z}$, hence $m = 1$, since $m \in \{1, \dots, n-1\}$. That is, for $\theta = \theta_0$ the function $|\eta_0|$ is only intersected by $|\eta_1|$. Furthermore, since all $|\eta_k|$ are continuous as well as differentiable on $(0, \pi/2)$ except the points where $|\eta_k| = 0$, and dominated by $|\eta_0|$ on $\big(0, \pi/(2n)\big)$, it holds that $1 = \eta_0 = |\eta_1| > |\eta_m|$ for $m \in \{2, \dots, n-1\}$ in θ_0.

For a given $k \in \{1, \dots, \lfloor n/2 \rfloor - 1\}$ it will now be assumed that for θ_{k-1} the dominating eigenvalue changes from η_{k-1} to η_k. In order to

prove (10) for the interval (θ_{k-1}, θ_k) it suffices to show that $|\eta_k|$ is not intersected by any other $|\eta_m|$ with $m \in \{0, \ldots, n-1\} \setminus \{k\}$.

According to Lemma 3.3 intersections may only occur for $\theta = \pi k/n$, which is the midpoint of the interval (θ_{k-1}, θ_k). Since

$$d_{k,m}\left(\frac{\pi k}{n}\right) \stackrel{!}{=} 0 \quad \Rightarrow \quad \sin\left(2\frac{\pi k}{n} - \pi\frac{k+m}{n}\right) \stackrel{!}{=} 0$$

implies $2\frac{\pi k}{n} - \pi\frac{k+m}{n} = \frac{\pi}{n}(k-m) \stackrel{!}{=} \nu\pi$, $\nu \in \mathbb{Z}$ and therefore $m = k$, the dominating function $|\eta_k|$ is not intersected by any other $|\eta_m|$ inside of (θ_{k-1}, θ_k).

Finally, (11) is shown by analyzing

$$d_{k,m}(\theta_k) = \sec^2\theta_k \, \sin\left(\pi\frac{k+1-m}{n}\right)\sin\left(\pi\frac{k-m}{n}\right) \stackrel{!}{=} 0\,.$$

The first sine becomes zero in the case of $m = k+1$. The second sine, which does not depend on θ, is nonzero due to $m \neq n-k$. Since the difference function changes its sign in θ_k, the dominating eigenvalue changes from η_k on the left of θ_k to η_{k+1} on the right as stated. $\Diamond$

4. Limit polygons and primes

In the case of $\theta > \pi/(2n)$, the absolute value of the dominating eigenvalue is greater than one causing the vertices of $z^{(\ell)}$ to tend to infinity if ℓ increases. Therefore, the polygons are scaled according to the following definition.

Definition 4.1. For $\theta \in (\theta_{k-1}, \theta_k]$, $k \in \{0, \ldots, \lfloor n/2 \rfloor\}$, with $\theta \neq \pi/2$ let

$$z_{s,\theta}^{(\ell)} := v_0 + \frac{1}{|\eta_k|^\ell}\big(z^{(\ell)} - v_0\big) = v_0 + \sum_{\mu=1}^{n-1}\left(\frac{\eta_\mu}{|\eta_k|}\right)^\ell v_\mu \tag{12}$$

be the sequence of polygons scaled according to the centroid of $z^{(0)}$ and the dominating eigenvalue with index k.

The rightmost representation of $z_{s,\theta}^{(\ell)}$ follows readily from (6). It also holds that $z^{(\ell)} = z_{s,\theta}^{(\ell)}$ in the case of $\theta \in \big(0, \pi/(2n)\big]$. That is, scaling has no effect in this case since the dominating eigenvalue is given by $\eta_0 = 1$. Based on the results obtained so far, a full classification of the behavior of the sequence $z_{s,\theta}^{(\ell)}$ for $\ell \to \infty$ can now be given.

Theorem 4.1. *For the base angle $\theta \in \big(0, \pi/2\big)$ and $\ell \in \mathbb{N}$, the scaled polygons $z_{s,\theta}^{(\ell)}$ tend to the limit polygons*
(13)

$$p_{s,\theta}^{(\ell)} := \begin{cases} v_0, & \text{if } \theta \in (0, \theta_0), \\ v_0 + \mathrm{e}^{\mathrm{i}\pi\ell/n} v_1, & \text{if } \theta = \theta_0, \\ v_0 + \mathrm{e}^{\mathrm{i}\pi k\ell/n} v_k, & \text{if } \theta \in (\theta_{k-1}, \theta_k),\ k \in \{1, \ldots, \lfloor n/2 \rfloor\}, \\ v_0 + \mathrm{e}^{\mathrm{i}\pi k\ell/n} v_k + \mathrm{e}^{\mathrm{i}\pi(k+1)\ell/n} v_{k+1}, & \text{if } \theta = \theta_k,\ k \in \{1, \ldots, \lfloor n/2 \rfloor - 1\}, \end{cases}$$

with θ_k given by (9). That is $\lim\limits_{\ell\to\infty} \left\| z_{s,\theta}^{(\ell)} - p_{s,\theta}^{(\ell)} \right\| = 0$, with $\|\cdot\|$ denoting the norm defined by $\|x\| = \sqrt{x^* x}$.

Proof. All four cases will be shown in the following manner. Based on the results of Lemma 3.4 the dominating terms, which lead to the definition of $p_{s,\theta}^{(\ell)}$, will be separated in the scaled decomposition (12) from a remaining finite distortion sum. The latter will tend to the zero vector if ℓ tends to infinity.

In the case of $\theta \in (0, \theta_0)$ the dominating eigenvalue is given by η_0 with the associated eigenpolygon $v_0 = p_{s,\theta}^{(\ell)}$. It follows readily from (6) that

$$\lim_{\ell\to\infty} \left\| z_{s,\theta}^{(\ell)} - p_{s,\theta}^{(\ell)} \right\| = \lim_{\ell\to\infty} \left\| \sum_{\mu=1}^{n-1} \eta_\mu^\ell v_\mu \right\| \le \sum_{\mu=1}^{n-1} \|v_\mu\| \underbrace{\lim_{\ell\to\infty} |\eta_\mu|^\ell}_{=0} = 0\,,$$

since $|\eta_\mu| < 1$ for $\mu \in \{1, \ldots, n-1\}$ according to Lemma 3.4.

In the case of $\theta = \theta_0 = \pi/(2n)$ the dominating eigenvalues are η_0 and η_1 with $\eta_0 = 1 = |\eta_1|$, where

$$\eta_1 = \sec\frac{\pi}{2n} \cos\left(\frac{\pi}{2n} - \frac{\pi}{n}\right) \mathrm{e}^{\mathrm{i}\pi/n} = \mathrm{e}^{\mathrm{i}\pi/n}\,.$$

Thus it can be stated that

$$z_{s,\theta_0}^{(\ell)} = v_0 + \eta_1^\ell v_1 + \sum_{\mu=2}^{n-1} \eta_\mu^\ell v_\mu = p_{s,\theta_0}^{(\ell)} + \sum_{\mu=2}^{n-1} \eta_\mu^\ell v_\mu\,.$$

Again, the distortion sum tends to the zero vector if ℓ tends to infinity since $|\eta_\mu| < 1$.

In the case of $\theta \in (\theta_{k-1}, \theta_k), k \in \{1, \ldots, \lfloor n/2 \rfloor\}$, it holds that

$$z_{s,\theta}^{(\ell)} = v_0 + \left(\frac{\eta_k}{|\eta_k|}\right)^\ell v_k + \sum_{\substack{\mu=1 \\ \mu\neq k}}^{n-1} \underbrace{\left(\frac{\eta_\mu}{|\eta_k|}\right)^\ell}_{\to 0} v_\mu\,. \tag{14}$$

At this, the eigenvalue representation (3) implies

$$\frac{\eta_k}{|\eta_k|} = \underbrace{\operatorname{sign}\left(\sec\theta\cos\left(\theta-\frac{\pi k}{n}\right)\right)}_{=1}\mathrm{e}^{\mathrm{i}\pi k/n} = \mathrm{e}^{\mathrm{i}\pi k/n}\,,$$

with $\theta \in (\theta_{k-1}, \theta_k)$, since the argument of the cosine factor varies within the interval $(-\pi/(2n), \pi/(2n))$. Replacing the obtained exponential representation of $\eta_k/|\eta_k|$ in (14) yields the limit polygon as stated in the third case of (13).

Finally, in the case of $\theta = \theta_k$, $k \in \{1, \ldots, \lfloor n/2 \rfloor - 1\}$ with the dominating eigenvalues η_k and η_{k+1} it holds that

$$z_{s,\theta_k}^{(\ell)} = v_0 + \underbrace{\left(\frac{\eta_k}{|\eta_k|}\right)^{\ell} v_k}_{=\mathrm{e}^{\mathrm{i}\pi k\ell/n}v_k} + \left(\frac{\eta_{k+1}}{|\eta_k|}\right)^{\ell} v_{k+1} + \sum_{\substack{\mu=1\\ \mu\neq k,k+1}}^{n-1} \underbrace{\left(\frac{\eta_\mu}{|\eta_k|}\right)^{\ell}}_{\to 0} v_\mu\,,$$

due to the results of the previous case for the second summand. In the case of the third summand it holds that

$$\frac{\eta_{k+1}}{|\eta_k|} = \underbrace{\operatorname{sign}\left(\sec\theta_k\cos\left(\theta_k-\frac{\pi(k+1)}{n}\right)\right)}_{=1}\mathrm{e}^{\mathrm{i}\pi(k+1)/n} = \mathrm{e}^{\mathrm{i}\pi(k+1)/n},$$

since the argument of the cosine function is $-\pi/(2n)$. $\Diamond$

It should be noted that the limit polygons $p_{s,\theta}^{(\ell)}$ depend on the iteration number ℓ due to the exponential coefficients of the eigenpolygons, which reflect the rotational effect of the transformation. Furthermore, only the counterclockwise oriented eigenpolygons v_k, with $k \in \{0,\ldots,\lfloor n/2 \rfloor\}$, are involved.

The following will now focus on the shapes of the limit polygons given by Th. 4.1 and therefore on the shapes of the eigenpolygons v_k, which are scaled Fourier polygons. The latter are depicted in Fig. 5 for $n \in \{3, \ldots, 6\}$ and $k \in \{1, \ldots, \lfloor n/2 \rfloor\}$. In this, circle markers indicate the scaled roots of unity lying on a circle with radius $1/\sqrt{n}$, whereas solid black markers indicate the vertices of the Fourier polygons. Also given is the vertex index or, in the case of multiple vertices, a comma separated list of indices. The case $k = 0$, where f_0 degenerates to one vertex with multiplicity n, is omitted.

The connections between eigenpolygons, prime numbers, and Euler's φ-function, where $\varphi(n)$ denotes how many of the numbers from 1 to n are relatively prime to n [8], are stated in the following theorem.

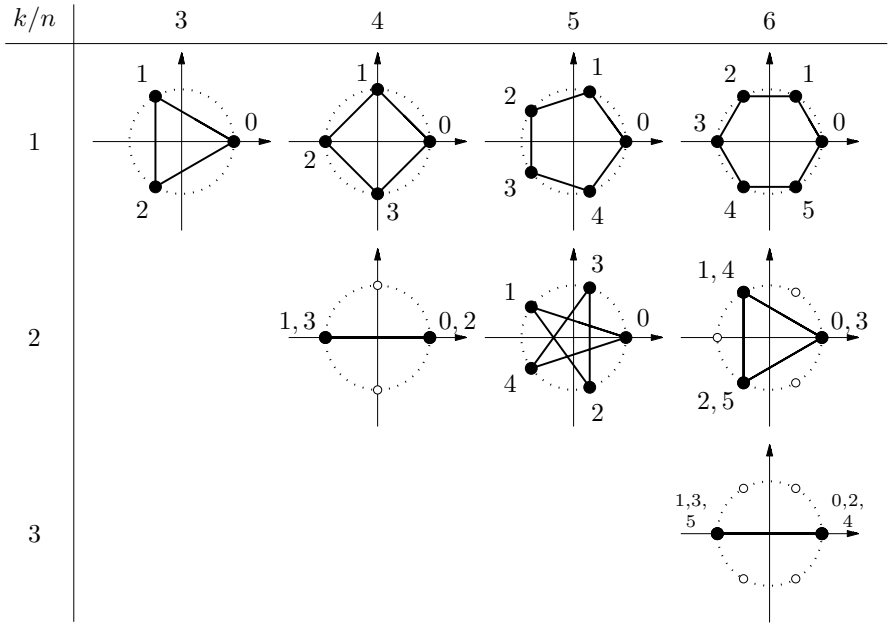

Figure 5: Fourier polygons f_k for $n \in \{3, \ldots, 6\}$ and $k \in \{1, \ldots, \lfloor n/2 \rfloor\}$.

Theorem 4.2. *Let* $\gcd(n,k)$ *denote the greatest common divisor of the two natural numbers* n *and* k*. Then the following holds for the eigenpolygons* v_k *and therefore for the limit polygons of* $z_{s,\theta}^{(\ell)}$ *in the case of* $\theta \in (\theta_{k-1}, \theta_k)$*,* $k \in \{1, \ldots, \lfloor n/2 \rfloor\}$*, and* $c_k \neq 0$*:*

1. *The eigenpolygon* v_k *is similar to the polygon obtained by successively connecting counterclockwise each* k*-th root of unity.*

2. *The eigenpolygon* v_k *is a* $\big(n/\gcd(n,k)\big)$*-gon with vertex multiplicity* $\gcd(n,k)$*.*

3. *The eigenpolygon* v_k *is a convex regular* (n/k)*-gon, if and only if* $k = \gcd(n,k)$*.*

4. *If* n *is a prime number, all eigenpolygons* v_k*, with* $k \in \{1,\ldots,\lfloor n/2 \rfloor\}$*, are* n*-gons. Using Euler's* φ*-function and* $q(n)$ *denoting the number of nonconvex* n*-stars in the sequence* v_k*,* $k \in \{2, \ldots, \lfloor n/2 \rfloor\}$*, this yields* $2q(n) + 2 = \varphi(n) = n - 1$*.*

5. *If* n *is odd, the first non* n*-star or regular* n*-gon eigenpolygon* v_k *counting backwards from* $\lfloor n/2 \rfloor$ *to zero occurs for* $k = \lfloor n/2 \rfloor - \lfloor p_1/2 \rfloor$*, where* p_1 *denotes the smallest prime factor in the factorization of* n*.*

Proof. The shape of the eigenpolygon v_k as described in item 1 follows

readily from Lemma 3.2.

To show item 2 let $m := \gcd(n,k)$, which results in the representations $n = m \cdot \hat{n}$ and $k = m \cdot \hat{k}$ with $\hat{n}, \hat{k} \in \mathbb{N}$. According to item 1, numbering n/m roots of unity by connecting each k root beginning with r^0 ends again in r^0, since

$$\left(\frac{n}{m} \cdot k\right) \bmod n = (\hat{n} \cdot m \cdot \hat{k}) \bmod n = (n \cdot \hat{k}) \bmod n = 0\,, \tag{15}$$

which implies $r^{nk/m} = r^0$. The following steps reproduce this polygon until each vertex has multiplicity m. Since m is the greatest common divisor, there is no larger divisor than m resulting in a polygon with less vertices.

To prove item 3, one can observe in the case of $k \neq \gcd(n,k)$ that according to (15) it takes $\hat{k}$ loops of roots of unity to return to r^0 leading to intersecting sides and therefore star shaped polygons, whereas in the case of $k = \gcd(n,k)$ one returns after n/k steps within one loop to r^0 thus leading to a convex polygon due to the geometry of the roots of unity.

Item 4 follows from the fact that $n \geq 3$ is prime and therefore $\gcd(n,k) = 1$ thus resulting in nonconvex n-stars according to the preceding results. Since v_0 represents the centroid and v_1 the regular n-gon, only the eigenpolygons v_k with $k \in \{2, \ldots, \lfloor n/2 \rfloor\}$ are relevant. This is also the reason for the summand 2 in the representation $2q(n) + 2 = \varphi(n) = n - 1$. The factor 2 of $q(n)$ comes due to the fact that $k \leq \lfloor n/2 \rfloor$.

Finally item 5 holds in the case of $n = p_1$ that is n is a prime number itself, since $k = 0$ and v_0 is the only non n-star or regular n-gon due to the first two items. Otherwise let $n = p_1 \cdots p_m$ be the factorization of n with odd prime factors $p_\mu \leq p_{\mu+1}$. It follows that

$$k = \lfloor n/2 \rfloor - \lfloor p_1/2 \rfloor = \frac{1}{2}(p_1 \cdots p_m - 1) - \frac{1}{2}(p_1 - 1) = p_1 \cdot \frac{p_2 \cdots p_m - 1}{2}\,,$$

which implies $\gcd(n,k) = p_1$ if n and the second factor on the right side have no common divisor greater than one. To prove the latter, it is assumed that there is a natural number $q > 1$ with $n = q \cdot \hat{n}$ and $p := (p_2 \cdots p_m - 1)/2 = q \cdot \hat{p}$ where $\hat{n}, \hat{p} \in \mathbb{N}$. Due to the representation of n, q has to be a product of some of the prime factors $p_2, \ldots, p_m$ and therefore is an odd number. Thus one can write

$$\hat{p} = \frac{p}{q} = \frac{1}{2} \underbrace{\frac{p_2 \cdots p_m}{q}}_{\in \mathbb{N},\ \text{odd}} - \underbrace{\frac{1}{2q}}_{\in (0,1/2)} \quad \Rightarrow \quad \hat{p} \notin \mathbb{N}$$

which contradicts the assumption $\hat{p} \in \mathbb{N}$. $\Diamond$

According to item 2 of Th. 4.2 the number n is a prime if, and only if, all $v_k = c_k f_k$, $c_k \neq 0$, hence all Fourier polygons f_k for $k \in \in \{2, \ldots, \lfloor n/2 \rfloor\}$ are star shaped n-gons, thus leading to a geometric primality check as depicted in Fig. 6. Columns containing only n-gons indicate that n is a prime number, whereas otherwise reduced polygons with vertex multiplicity greater one occur.

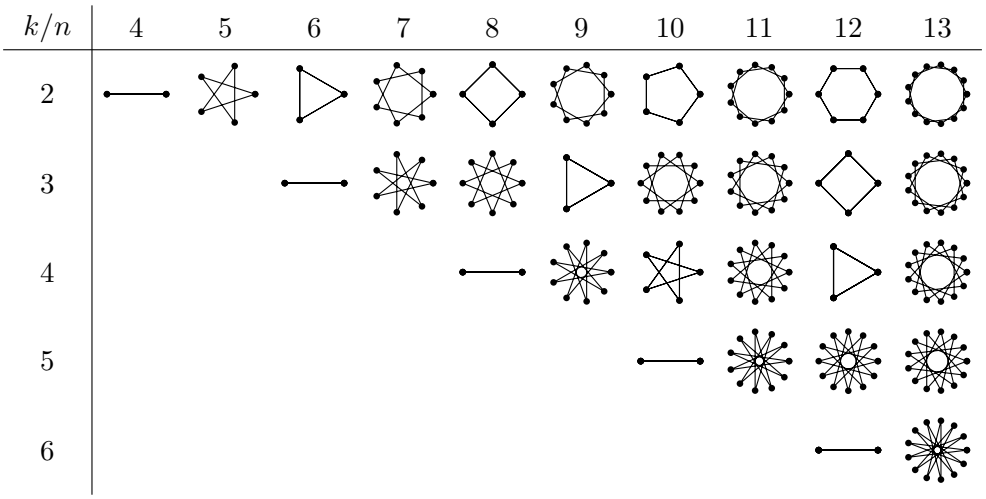

Figure 6: Fourier polygons f_k for $n \in \{4, \ldots, 13\}$ and $k \in \{2, \ldots, \lfloor n/2 \rfloor\}$.

Since $\nu \in \mathbb{N}$ is a factor in the factorization of each ν-th number, the according ν-gon appears in the associated column. That is, each second column contains a 2-gon, each third a 3-gon and so on. Hence, the associated numbers n are no prime numbers, thus leading to a geometric interpretation of the arithmetic sieve of Eratosthenes.

In addition, the items 2 and 5 of Th. 4.2 lead to the following geometric prime factorization algorithm joining the family of factorization techniques [9]. If n is even, it is iteratively divided by two until the remaining number $\tilde{n}$ is odd. For this number the Fourier polygons f_k starting from $k = \lfloor \tilde{n}/2 \rfloor$ backwards are examined. In the case of $k > 0$, the first non $\tilde{n}$-star or regular $\tilde{n}$-gon reveals the smallest prime factor as

$p_1 = 2\,(\lfloor \tilde{n}/2 \rfloor - k) + 1$. Furthermore, according to item 2, f_k is a $(\tilde{n}/p_1)$-gon. Therefore, one can set $\tilde{n}$ to this new value and start again to collect the prime factors of the remainder. The algorithm stops, if $\tilde{n}$ is a prime number, which results in $k = 0$.

The angles given by the exponential factors in the definition (13) of the scaled limit polygons reveal the rotational effect of the transformation. They depend not only on the number n of vertices and ℓ of iterations, but also on the index k of the associated eigenpolygon thus leading to more symmetries as stated in the following theorem.

Theorem 4.3 *The limit polygons $p_{s,\theta}^{(\ell)}$ differ for odd and likewise for even iteration numbers ℓ only in a counterclockwise cyclic shift of vertex indices, but not in geometry. More precisely, it holds that*

$$\left(p_{s,\theta}^{(\ell)}\right)_{(\mu+1) \bmod n} = \left(p_{s,\theta}^{(\ell+2)}\right)_{\mu}\,, \tag{16}$$

where $\ell \in \mathbb{N}$, $\mu \in \{0, \ldots, n-1\}$. Furthermore, for $\theta \in (\pi/(2n), \pi/2)$ the sequence of scaled polygons $z_{s,\theta}^{(\ell)}$ contains $2n$ converging subsequences with

$$\lim_{\ell \to \infty} z_{s,\theta}^{(2n\ell+\nu)} = p_{s,\theta}^{(\nu)}\,, \tag{17}$$

where $\nu \in \{0, \ldots, 2n-1\}$.

Proof. Since $p_{s,\theta}^{(\ell)}$ is a linear combination of rotated eigenpolygons, it suffices to show that (16) holds for each summand, that is

$$\left(\mathrm{e}^{\mathrm{i}\pi k\ell/n} v_k\right)_{(\mu+1) \bmod n} = \left(\mathrm{e}^{\mathrm{i}\pi k(\ell+2)/n} v_k\right)_{\mu}\,,$$

where $k \in \{1, \ldots, n-1\}$. Using Lemma 3.2 and the definition of the root of unity $r = \exp(2\pi\mathrm{i}/n)$ this follows from

$$\mathrm{e}^{\mathrm{i}\pi k\ell/n}\,(v_k)_{(\mu+1) \bmod n} = \mathrm{e}^{\mathrm{i}\pi k\ell/n} r^k\,(v_k)_{\mu} = \mathrm{e}^{\mathrm{i}\pi k(\ell+2)/n}\,(v_k)_{\mu}\,.$$

Since in the case of $k = 0$ all entries of v_0 are the same this implies (16).

Equation (17) follows from the $2n$-periodicity of the exponential factors given by the definition of $p_{s,\theta}^{(\ell)}$ according to (13), that is $\mathrm{e}^{\mathrm{i}\pi k(2n\ell+\nu)/n} = \mathrm{e}^{\mathrm{i}\pi k\nu/n}$ for $\nu \in \{0, \ldots, 2n-1\}$. $\Diamond$

In the case $\theta \in (\theta_{k-1}, \theta_k)$, $k \in \{1, \ldots, \lfloor n/2 \rfloor\}$, the limit polygon is a rotated and scaled Fourier polygon with preserved centroid similar to those depicted in Fig. 5. In contrast, for $\theta = \theta_k$, $k \in \{0, \ldots, \lfloor n/2 \rfloor - 1\}$ there are two possible limit polygons each a linear combination of up to two eigenpolygons shifted by the centroid.

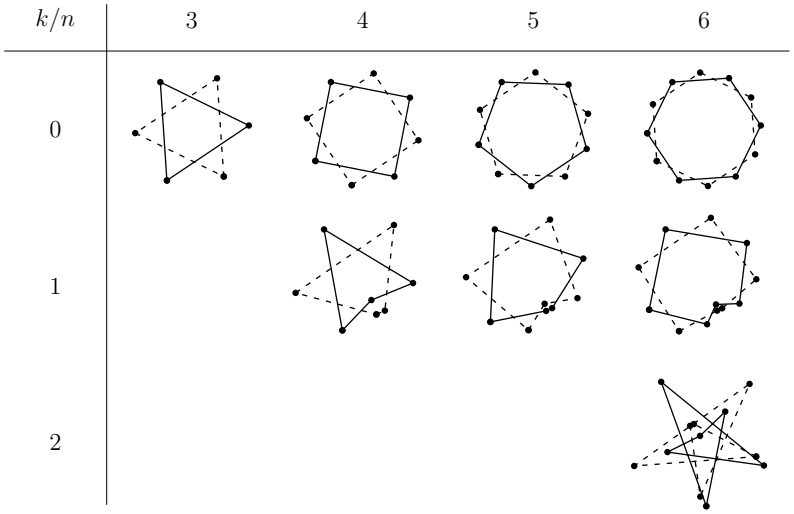

Figure 7: Limit polygons for $n \in \{3, ..., 6\}$, $\theta = \theta_k$, $k \in \{0, ..., \lfloor n/2 \rfloor - 1\}$. Drawn through lines and dashed lines indicate limits for subsequences with odd and even ℓ respectively.

For $(z^{(0)})_\mu := (\mu+1)\exp(\mathrm{i}\pi\mu/(5n))$, $n \in \{3, \ldots, 6\}$, $\mu \in \{0, \ldots, n-1\}$, and $k \in \{0, \ldots, \lfloor n/2 \rfloor - 1\}$ the resulting two limit polygons are depicted in Fig. 7. Drawn through lines and dashed lines indicate limits for subsequences with odd and even ℓ respectively. In particular the first row contains two regular n-gons rotated by angle π/n, which is half the angle of the according root of unity.

The first case in Fig. 7, that is $n = 3$, $k = 0$ and therefore $\theta = \pi/6$, represents Napoleon's theorem. In particular, since $\eta_0 = |\eta_1| = 1$ and $\eta_2 = 0$ the distortion sum $z^{(\ell)}_{s,\theta} - p^{(\ell)}_{s,\theta}$ is the zero vector for all ℓ. Therefore one step suffices to generate a regular triangle. From that point on, according to Th. 4.3, further iterations lead to a sequence of two alternating dual triangles which are depicted in the table.

In the case of $n > 3$, $k = 0$ the distortion sum is nonzero, hence there is only one Napoleon. But since the error decreases by powers of the eigenvalue quotients this leads to a fast convergence and therefore asymptotically also to alternating dual regular n-gons.

In the following, an overview of properties of the unscaled iterative polygon transformation is given, which can now be readily derived from the results obtained so far.

Corollary 4.1. *The following holds:*

1. *For $\theta \in \big(0, \pi/(2n)\big)$ the concentric polygons $z^{(\ell)}$ degenerate to their common centroid if ℓ tends to infinity.*

2. *In the case of $\theta = \pi/(2n)$ the sequence $z^{(\ell)}$ consists of bounded polygons which become regular if ℓ tends to infinity.*

3. *For $\theta \in \big(\pi/(2n), \pi/2\big)$ the vertices of $z^{(\ell)}$ tend to infinity as ℓ grows. In this, the limit polygons given by Th. 4.1, scaled with respect to the centroid by the ℓ-th power of the eigenvalue with the largest absolute value, represent the dominating terms thus the asymptotical behavior.*

Proof. The items 1 and 2 follow due to $z^{(\ell)} = z^{(\ell)}_{s,\theta}$ since $\theta \in (0, \pi/(2n)]$ and the results given by Th. 4.1. Likewise item 3, where $z^{(\ell)}_{s,\theta}$ differs from $z^{(\ell)}$ just in the scaling by $|\eta_k|$, which is greater than one because of $\theta > \pi/(2n)$ and the results given by Lemma 3.4. It should be noted that in this case the distortion sum may also grow to infinity, since the absolute values of other eigenvalues might be greater than one. Nevertheless, due to the scaling by powers of eigenvalues, the dominating eigenvalue(s) define the behavior of the sequence $z^{(\ell)}$ if ℓ tends to infinity. $\Diamond$

5. Conclusion

A full classification of the limit figures obtained by successively iterating the process of generating a new polygon by taking the apices of similar isosceles triangles erected on the sides of the preceding polygon has been presented. All characteristic base angles leading to a change in the geometry of the limit polygon have been determined. Additionally, it has been shown that these limit polygons are linear combinations of eigenpolygons of the initial polygon. Since all transformation schemes which can be represented by circulant matrices lead to the same eigenpolygons, the results obtained in this paper are not only applicable to the analyzed transformation, but to a broad variety of geometric polygon transformations. In particular, the symmetric properties of the eigenpolygons imply a connection to prime numbers and therefore lead to a geometric sieve as well as factorization method for prime numbers.

Beyond the beauty of geometry and its connection to number theory lies the applicability of such transformations, which, at first sight, might not be obvious. For example, the regularizing effect of similar transformations can be used in mesh smoothing as proposed by the au-

thors in [15, 16, 18]. Finally, the transformation process can be generalized in many ways, like the use of different base angles θ for different sides leading to different symmetries, the use of non isosceles triangles or the use of iteration step dependent base angles $\theta(\ell)$. Additionally, it would be interesting to consider such iterated polygon transformations in non-Euclidean geometries and to analyze the deeper link between group theory and such transformations.

Acknowledgment. I would like to thank my colleagues at NIKI Ltd., Aristos Tzavellas, Theodoros Athanasiadis and Vivi Zapsa, for their support during the development of this paper's initial ideas with critical comments, numerical tests and visualization.

Dimitris Vartziotis

References

[1] BERLEKAMP, E. R., GILBERT, E. N. and SINDEN, F. W.: A polygon problem, *Amer. Math. Monthly* **72** (1965), 233–241.

[2] DAVIS, P. J.: Circulant Matrices, 2nd ed., Chelsea Publishing, New York, 1994.

[3] FOX, M.: Napoleon triangles and adventitious angles, *Math. Gazette* **82** (1998), 413–422.

[4] GRAY, R. M.: Toeplitz and circulant matrices: a review, *Found. Trends Commun. Inf. Theory* **2** (2006), 155–239.

[5] GRAY, S. B.: Generalizing the Petr–Douglas–Neumann theorem on n-gons, *Amer. Math. Monthly* **110** (2003), 210–227.

[6] MERRIELL, D.: Further remarks on concentric polygons, *Amer. Math. Monthly* **72** (1965), 960–965.

[7] PECH, P.: The harmonic analysis of polygons and Napoleon's theorem, *J. Geom. Graph.* **5** (2001), 13–22.

[8] RIBENBOIM, P.: The little book of bigger primes, 2nd ed., Springer, New York, 2004.

[9] RIESEL, H.: Prime numbers and computer methods for factorization, 2nd ed., Birkhäuser, 1994.

[10] SCHUSTER, W.: Regularisierung von Polygonen, *Math. Semesterber.* **45** (1998), 77–94.

[11] SHAPIRO, D. B.: A periodicity problem in plane geometry, *Amer. Math. Monthly* **91** (1984), 97–108.

[12] SHEPHARD, G. C.: Sequences of smoothed polygons, In: Discrete Geometry, András Bezdek (ed.), Marcel Dekker Inc., 2003, 407–430.

[13] VARTZIOTIS, D.: TWT Newsletter: Special issue on the relation between polygon transformations and prime numbers, TWT GmbH Science & Innovation (2007).

[14] VARTZIOTIS, D.: Problem 11328, *Amer. Math. Monthly* **114** (2007), 925; BATAILLE, M.: Solution, **116** (2009), 656.

[15] VARTZIOTIS, D., ATHANASIADIS, T., GOUDAS, I. and WIPPER, J.: Mesh smoothing using the geometric element transformation method, *Comput. Methods Appl. Mech. Eng.* **197**/45–48 (2008), 3760–3767.

[16] VARTZIOTIS, D. and WIPPER, J.: The geometric element transformation method for mixed mesh smoothing, *Eng. Comput.* **25**/3 (2009), 287–301.

[17] VARTZIOTIS, D. and WIPPER, J.: On the construction of regular polygons and generalized Napoleon vertices, *Forum Geom.* **9** (2009), 213–223.

[18] VARTZIOTIS, D., WIPPER, J. and SCHWALD, B.: The geometric element transformation method for tetrahedral mesh smoothing, to appear in *Comput. Methods Appl. Mech. Eng.*, `http://dx.doi.org/10.1016/j.cma.2009.09.027`

[19] WETZEL, J. E.: Converses of Napoleon's theorem, *Amer. Math. Monthly* **99** (1992), 339–351.

[20] ZIV, B.: Napoleon-like configurations and sequences of triangles, *Forum Geom.* **2** (2002), 115–128.